Analyst

PAPER

View Article Online
View Journal | View Issue

Cite this: *Analyst*, 2025, **150**, 5445

Toward minimally invasive metabolomics: GC-MS metabolic fingerprints of dried blood microsamples in comparison to plasma

Daniel Marques de Sá e Silva, †[a,b] Marlene Thaitumu,†[b,c] Christina Virgiliou,[b,d] Alexandra Tiganouria,[a,b] Fernanda Rey-Stolle,[e] Glykeria Avgerinou,[f] Anatoli Petridou,[f] Vasileios Mougios,[f] Georgios Theodoridis[a,b] and Helen Gika *[b,c]

Received 2nd September 2025,
Accepted 20th October 2025

DOI: 10.1039/d5an00937e

rsc.li/analyst

Global metabolic profiles of dried blood microsamples (BμS) were studied in comparison to conventional plasma and blood samples using Gas Chromatography-Mass Spectrometry (GC-MS). Venous blood from 10 healthy, overnight-fasted individuals was collected and used to produce dried microsamples on Whatman cards, Capitainer and Mitra devices. In parallel paired plasma samples were collected. The metabolite extraction protocol was optimized and methanol was selected as the extraction solvent. Twenty μL of the venous BμS and plasma were analyzed using the Fiehn GC-MS protocol which includes methoximation and trimethylsilylation derivatization steps. In an additional study, three paired finger capillary BμS (Mitra), liquid venous blood, and plasma metabolic profiles were evaluated. BμS devices, mainly the Mitra, provided equivalent or greater information than plasma, considering it had the highest mean abundance of features and most annotated metabolites (37) with highest abundance. Additionally, in the last study, 14 metabolites had statistically higher abundance in the capillary blood Mitra BμS compared to liquid venous blood and plasma. Overall, the results suggest that BμS is a viable alternative for untargeted blood metabolomics, providing comparable information. Since the different BμS devices capture different metabolic profiles, the choice of device for a research study should be carefully considered depending on one's goals.

1 Introduction

In recent decades, omics disciplines, which comprehensively profile endogenous molecules in biological specimens, have emerged as rapidly advancing fields within bioanalysis. Among these, metabolomics, the systematic study of small-molecule metabolites involved in biochemical pathways, has attained significant prominence as a critical tool for elucidating cellular phenotypes and metabolic states.[1,2] Metabolomic blood analysis holds great promise for clinical laboratory applications by enhancing diagnostic efficiency and enabling more comprehensive disease risk assessment, areas where current diagnostics often fall short. Thanks to advances in analytical and computational methods, a mere microliter of blood (≤1 μL) is now sufficient for comprehensive metabolic profiling. This renders blood microsampling (BμS) techniques an attractive asset in metabolomics as they also offer many other advantages. It is a minimally invasive, cost-effective approach allowing sample collection outside clinical settings, including at home.[3–5]

Dried Blood Spots (DBS), the oldest form of BμS, have been applied for decades in numerous analyses[6–8] with a main focus on diagnosing infections and the screening for inborn errors of metabolism.[9] However, recently, new and innovative BμS technologies have emerged overcoming some of the DBS drawbacks, such as hematocrit bias.[10] New quantitative BμS devices offer high accuracy in collection volume and analytical precision, both critical features for metabolic profiling studies and targeted metabolomics.

Since the first use of GC-MS to measure derivatized fatty acids in DBS,[11] GC-MS analysis of BμS has evolved within the

[a]*School of Chemistry, Aristotle University of Thessaloniki, 54124 Thessaloniki, Greece. E-mail: dmarque@auth.gr, gtheodor@chem.auth.gr, atiganoa@chem.auth.gr*
[b]*Biomic AUTh, Center for Interdisciplinary Research and Innovation (CIRI-AUTH), Balkan Center, B1.4, 12 57001 Thessaloniki, Greece. E-mail: cvirgiliou@cheng.auth.gr*
[c]*School of Medicine, Aristotle University of Thessaloniki, 54124 Thessaloniki, Greece. E-mail: mthai@auth.gr, gkikae@auth.gr*
[d]*Department of Chemical Engineering, Aristotle University of Thessaloniki, Thessaloniki 54124, Greece*
[e]*Centro de Metabolómica y Bioanálisis (CEMBIO), Facultad de Farmacia, Universidad San Pablo-CEU, CEU Universities, Urbanización Montepríncipe, 28660 Boadilla del Monte, Madrid, Spain. E-mail: frstolle@ceu.es*
[f]*School of Physical Education & Sport Science at Thessaloniki, Aristotle University of Thessaloniki, 57001 Thessaloniki, Greece*
† Authors with equal contribution.

field of metabolomics.[12] However, even though GC-MS delivers broad metabolite coverage across central metabolism – offering both high separation quality and rich identification capacity – mostly LC-MS-based metabolic profiling has been applied in BμS.[13–17] To date only a few GC-MS metabolomics studies have been conducted on BμS,[18–22] and just three of these have been focused on the comparison of BμS to conventional blood sample metabolic profiles.[20–22] The latter aimed to investigate if BμS could reliably substitute for whole blood and plasma, in GC-MS-based untargeted metabolomic profiling, offering benefits in stability, convenience, and biomarker detection. In general, comparable detection and identification numbers were observed with only some specific metabolites showing different trends. Kong *et al.* reported as an example that some metabolites are underrepresented in DBS and that lysine, citric acid and adenosine monophosphate (AMP) were uniquely detected in plasma or blood.[22] In another study applying GC-MS to compare metabolic profiles of DBS from finger prick, DBS from venous blood, whole blood and plasma from sixteen healthy volunteers, it was found that the number of detected metabolites was similar with only less than 15% differential metabolite detection specific to each matrix.[21] Similar observations have been reported also when DBS and Mitra GC-MS metabolic profiles were compared with that of blood in a case study of breast cancer patients. The data provided comparable results in terms of metabolite detection capabilities and suggested that BμS was effective in detecting disease-related metabolic changes.[20]

Although previous studies have highlighted valuable insights into the potential of these sampling approaches, they completely overlook critical technical aspects, particularly how the choice of extraction protocol influences metabolic coverage. This lack of detailed methodological information has limited our understanding of the true capabilities and limitations of BμS, underscoring the urgent need for systematic evaluation, which is what the present study addresses.

In the present study, the untargeted GC-MS profiles of different devices under different extraction conditions were tested, aiming to obtain the most comprehensive profile possible. Finally, the profiles obtained from capillary blood collected using the Mitra BμS device and the paired plasma and whole blood from three individuals were studied. To the best of our knowledge, this is the first comprehensive study comparing global metabolic profiles from three different BμS devices against plasma and venous liquid blood using GC-MS, broadening the coverage of LC-MS metabolome obtained as a continuation of our previous work.[16]

2 Materials & methods

2.1 Chemicals and reagents

All solvents used were of LC-MS grade. Acetonitrile (ACN) and methanol (MeOH) were acquired from VWR BDA Chemicals (Radnor, PA). Myristic-d_{27} acid, fatty acid methyl esters (FAME) standard mix, pentadecane, methoxyamine hydrochloride, and pyridine were purchased from Sigma Aldrich (St Louis, MO, USA). *N*-Trimethylsilyl-*N*-methyl trifluoroacetamide (MSTFA) was obtained from Restek corporation (PA, USA) and trimethylchlorosilane (TMCS) from Alfa Aesar (Leicestershire, UK). Ultrapure water was produced using a Hydrolab demineralizer (Straszyn, Poland).

2.2 Microsampling devices

Twenty-microliter (two 10 μL spots per card) Capitainer® B cards were purchased from Capitainer (Solna, Sweden). 20 μL Mitra devices were acquired from Neoteryx (Torrance, CA). Whatman protein saver cards, each containing five collection spots, were obtained from Sigma-Aldrich (St Louis, MI).

2.3 Blood sample collection & handling

Venipuncture blood was collected by a trained phlebotomist from ten (five men and five women) healthy overnight-fasted individuals. The collection was undertaken after written informed consent. All experiments were performed in accordance with the guidelines of the Declaration of Helsinki. The study was approved by the Research and Ethics Committee of the Aristotle University of Thessaloniki (#306272/2022). Antecubital venipuncture blood from each individual was collected in two 6 mL EDTA tubes. 20 μL of the blood was pipetted onto Whatman DBS cards. A drop of the blood was applied on each of the two spots of the Capitainer B cards using a Pasteur pipette. For Mitra collection, the tip was partially dipped in the EDTA tube for ~6 seconds. A portion of the venipuncture blood was also separated for plasma collection. The BμS samples were left to dry at room temperature for 3 hours (h) before storage at −80 °C in desiccant pouches until analysis; plasma and liquid venous blood were also stored at −80 °C until analysis. A schematic diagram of the study design is illustrated in Fig. 1.

2.4 Analytical sample preparation and derivatization

2.4.1 Preparation of reagents and standards. Myristic-d_{27} acid stock solution was prepared by dissolving 1 mg of the standard in 1 mL of pyridine and diluting tenfold to make a 100 mg L^{-1} solution. Methoxyamine (MEOX) stock solution was prepared by dissolving 40 mg in 1 mL of pyridine to prepare a 40 mg mL^{-1} solution. Pentadecane solution was prepared by dissolving 130.2 μL of pentadecane in 1 mL of pyridine and diluting sixteenfold to make a 6.25 mg L^{-1} solution. MSTFA was prepared with 1% chlorotrimethylsilane (TMCS); for a 10 mL stock solution, 0.1 mL of TMCS was added to 9.9 ml MSTFA.

2.4.2 Sample preparation and derivatization

2.4.2.1 Liquid venous blood. Liquid venous blood samples from the ten individuals were left to thaw at 4 °C. The samples were vortexed and 50 μL was transferred to separate Eppendorf tubes. 10 μL of the internal standard (ISTD) myristic-d_{27} acid was added to each sample followed by 140 μL of ACN–MeOH 70 : 30 (v/v). This derivatizable internal standard was added prior to the derivatization step to correct for variations in extraction, derivatization efficiency, and injection, ensuring

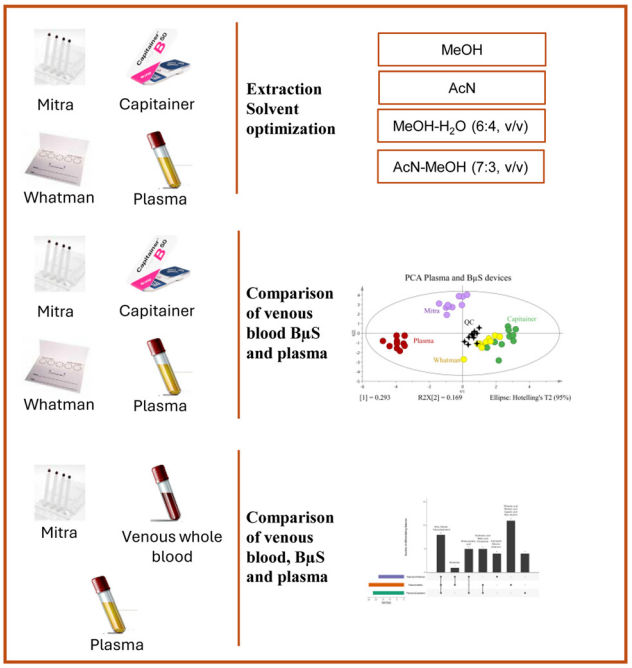

Fig. 1 Schematic of the study design.

accurate quantification of target metabolites. The samples were briefly vortexed for 10 min. Afterwards, the samples were centrifuged at 6720*g* for 10 min at 4 °C. All the supernatant was transferred to glass vials and evaporated using a speed vacuum concentrator.

The Fiehn methoxymation–trimethylsilylation derivatization protocol was applied[23,24] as follows. First, 10 μL of methoxyamine (MeOX) (40 mg mL^{-1} in pyridine) was added – to protect ketone groups – and the samples were briefly vortexed and incubated for 90 min at 30 °C. In the second step, 90 μL of 1%-TMCS in MSTFA was added, the samples were vortexed and incubated for 30 min at 37 °C. The MSTFA reacts with molecules containing acidic protons which are common in carboxyl, hydroxyl, amino, imino, and sulfuryl groups thus making them non-polar and reducing their boiling point.[24] As a final step, 10 μL of 6.25 mg L^{-1} pentadecane was added as a second internal standard, to assess analytical precision. It is used to assess the quality of the data and correct for variations in injection and signal abundance if necessary. The samples were loaded on the autosampler and left for six hours before injection in order to ensure complete derivatization.[25] QC samples were prepared using pooled liquid venous blood from the ten individuals. The QC samples were prepared using the same protocol detailed above and injected five times within the run, after every two injections. Initial trials on extraction optimization were performed in a pool sample.

2.4.2.2 BμS extraction optimization. Four different extraction solvents were evaluated, *i.e.* MeOH, ACN, MeOH–H_2O 60 : 40 (v/v), and ACN–MeOH 70 : 30 (v/v) on each device, in triplicate. Either one Mitra tip (20 μL), one Whatman spot (20 μL) or two Capitainer discs (each 10 μL), prepared with pooled blood were placed in 1.5 mL Eppendorf tubes and hydrated using 20 μL of H_2O. 10 μL of the ISTD myristic-d_{27} acid was added to the Eppendorf, followed by 300 μL of one of the extraction solvents. The samples were briefly vortexed and sonicated for 10 minutes (min). Afterwards, the devices were removed with tweezers, and the tubes were centrifuged (6720*g* for 10 min at 4 °C). The supernatants (290 μL) were transferred to clean glass vials and evaporated using a speed vacuum concentrator (Eppendorf Concentrator plus, Stevenage, United Kingdom).

The samples were derivatized by applying the same protocol as previously described.[23,24] The samples were loaded on the autosampler and left for six hours before injection in order to ensure complete derivatization.[25] QC samples were prepared by mixing aliquots of the final extract from all the samples and injecting one QC after every five samples.

2.4.2.3 Venous BμS vs. plasma comparison. Samples from the ten individuals collected using the three BμS devices and plasma (20 μL) were extracted using the procedures described above with 320 μL of the extraction solvent selected as optimum, namely MeOH. After extraction, 85 μL of supernatant from each sample was aliquoted into three separate vials (n = 3 technical replicates). An additional 45 μL of supernatant from each sample was collected and mixed to prepare within-run QC. 85 μL (equal volume as the samples) of the QC mix was aliquoted into separate QC vials (same volume as the samples). The samples were evaporated and stored at −80 °C before derivatization. Derivatization was performed on the day of analysis based on randomized sequence. The derivatization protocol was as previously described albeit with one-third of the reagent volumes, given the reduced sample volume per replicate/vial. Accordingly, double the amount (20 μL) of the check standard pentadecane (diluted fourfold) was added after the derivatization before loading on the instrument. Like previously, injection was delayed for six hours to ensure derivatization was complete.

2.4.2.4 Capillary BμS vs. blood and plasma comparison. Plasma, venous blood and BμS with capillary blood were collected from 3 individuals. Plasma and venous blood were acquired through phlebotomy, while capillary blood was collected from a finger prick using Mitra tips, following manufacturer's instructions. 20 μL of plasma, whole blood and the Mitra tip were added to the Eppendorf tubes and extracted as described above. QC samples were also prepared as described in Section 2.4.2.2. Derivatization was performed on the day of analysis based on randomized sequence. Derivatization and addition of the internal standard (pentadecane) were carried out as described in session 2.4.2.2. Likewise, injection was delayed for six hours to ensure derivatization was complete.

2.5 GC-MS analysis

A Bruker EVOQ-456 GC-MS coupled with a PAL RSI autosampler was used. Separation was performed using a non-polar DBS-5 capillary column (5% – phenyl-methyl-polysiloxane) with helium as the carrier gas. The flowrate was 1.1 mL min^{-1}. A PTV injector was used with the inlet temperature initially held at 110 °C for 1 minute (min), then ramped to 250 °C at

720 °C min^{-1}; the temperate was held at 250 °C for 12 min before being decreased back to 110 °C at 720 °C min^{-1}; where it was maintained until the end of the run. Injection was set in spitless mode from 0 to 5 min and then in split mode from after 5 min with a 10 : 1 split ratio. A solvent delay of 6.8 min was applied.

The oven temperature program was as follows: the initial temperature was held for 1 min at 60 °C, then ramped to 320 °C with 10 °C min^{-1} rate; it was then held at 320 °C for 10 min and then dropped to 60 °C, where it was held for 1 min until the end of the run.

The GC-MS was operated in full scan in MS mode at a 50–600 *m*/*z* scan range with a 500 ms scan time. Electron (EI) ionization was applied with a source temperature at 230 °C and the transfer line temperature at 250 °C.

2.6 Data analysis

For the solvent optimization and device comparison, pre-processing of the data was performed using MSDIAL (version 4.9.221218). The comparison of capillary BμS devices with whole blood and plasma was pre-processed in XCMS (version 4.3) in R (version 4.3.0), following the "Metabonaut" workflow.[26] In MS-DIAL, raw data files were processed directly, whereas in XCMS, data were first converted to the .mzml format using Proteowizard MSConvert (version 3.0.23129). Detailed parameter settings for all data processing steps are provided in the SI.

Identification of features (a detected metabolite with a specific paired *m*/*z* and rt) was performed using multiple software in order to optimize the number of annotations and for confirmation purposes: AMDIS (version 32) and MSDIAL (version 4.9.221218). For AMDIS analysis, the raw data were first converted to .cdf files using NetCDF software and the spectra were matched against the NIST spectral library. The results were later manually curated using application "GAVIN3" under MATLAB (version R2024a). For the deconvolution parameters a minimum matching factor of 80 was used for all detected features. On MSDIAL, two libraries, Fiehn BinBase DB (Rtx5-Sil MS, FAMEs-based RI) and RIKEN DB (Rtx5-Sil MS, predicted Fiehn RI) were used for annotations. To perform Retention Index (RI) matching, a FAMEs mixture was injected during the analytical sequence. Retention times (RT) of the FAMEs were fitted to their reference RI values from the NIST library using a polynomial function. This calibration curve was then applied to assign RI values to the annotated compounds for identity confirmation (SI Table S1).

2.7 Statistical analysis

Deconvoluted data were first analyzed in MS Excel (version 2405) and normalization was performed using a linear model based on QC response at QC MXP software.[27] Principal component analysis (PCA) and supervised orthogonal partial least-square discriminant analysis (PLS-DA) were performed using Simca (version 14.1). Data for the multivariate analysis was normalized and filtered for imprecision (QC features with >30% CV excluded). Data were log transformed, pareto scaled and missing values were imputed using the *k*-nearest neighbors (*k*NN) method (k = 3). Univariate data analysis was performed using MS Excel (version 2405) on log-transformed features abundance (peak area) with <30% coefficient of variance (CV) in QCs. Multiple hypothesis testing was performed using the two-stage linear step-up procedure of Benjamini, Krieger, and Yekutieli (BKY) with a false discovery rate (FDR) of 0.5% in Prism – GraphPad (version 10).[27,28]

3 Results and discussion

3.1 Liquid venous blood analysis

Based on the analysis of liquid venous blood from ten individuals, a library of identified metabolites was built with the aim of serving as a reference and to identify and annotate metabolites from the study cohort. Fifty-seven metabolites were identified including amino acids and their derivatives, organic acids, sugars, and long chain fatty acids as can be seen in the SI Table S2, which provides the list of annotated metabolites in blood and EI-generated fragments matching those in the reference library for each compound. Annotation confidence levels were assigned adapted from Sumner *et al.*[29] Level 1 identifications were confirmed by matching both retention time and electron ionization (EI) spectra with authentic standards, while level 2 annotations were based solely on EI spectral similarity. To further enhance annotation confidence, retention index (RI) matching was also performed, as shown in SI Table S1. The EI-generated fragments that matched those in the reference library are listed in SI Table S2.

A particular challenge in the GC-MS analysis of carbohydrates is the formation of multiple derivatives during trimethylsilylation, resulting from the various tautomeric forms of sugars.[30] Additionally, the presence of multiple structural isomers often leads to highly similar fragmentation patterns, making their differentiation difficult. Consequently, the level 2 annotations of sugars reported in this study should be interpreted with caution.

3.2 BμS solvent extraction selection

To explore the most appropriate solvent for metabolite extraction from the dried blood samples, a pooled sample was extracted using two pure solvents, MeOH and ACN; and two solvent mixtures, MeOH–H_2O 60 : 40 (v/v) and ACN–MeOH 70 : 30 (v/v). These were chosen based on our group's earlier publications.[20–22] To evaluate the efficiency of the extraction solvents for this type of analysis, we considered the total number of extracted features, the overall features abundance, and the precision of analysis per extract.

BμS devices containing pooled blood extracts using the four different solvents were analyzed by a single run in a randomized order. Evaluation of the QC's precision using R^2 correlation of QC features intensities revealed no significant signal variation across the run. As well as that, IS signals (Myristic acid d-27 and pentadecane), were checked to address signal drifts. Therefore, no normalization protocol was applied for

this experiment. Additional evidence to support such an approach can be found in SI Table S3.

For the evaluation of the number of features, only those with signal detected in at least two out of three replicates were considered. Based on these data, it was found that the highest number of features was detected using MeOH in two out of the three cases (149 in Whatman and 193 in Capitainer). For the Mitra device, the solvent yielding the highest number of features was ACN–MeOH 70 : 30 (v/v) (216 features) followed closely by MeOH (187 features). ACN–MeOH 70 : 30 (v/v) yielded the second highest number of features for Whatman (125 features), and MeOH–H_2O 60 : 40 (v/v) was the second best for Capitainer (156 features). A graphical illustration of the number of detected features per extraction solvent and BμS is shown in Fig. 2 where abundance in color corresponds to increase in the number of detected features. As can be seen, Whatman yielded fewer features than the two other devices, regardless of the solvent used. Venn diagrams displaying how many features were unique and common between the solvents in each BμS device are shown in Fig. S1.

Regarding the overall abundance of the detected features (signals detected in at least two out of three replicates), MeOH appeared to be the most efficient. A comparison of the features abundance per solvent extract and BμS device can be seen in Fig. 3. In the figure the color represents the sum abundance of all features in a given solvent, after averaging the values found in the triplicates. In addition to producing the highest number of extracted features, MeOH also yielded the greatest total abundance across all three devices. MeOH–H_2O 60 : 40 (v/v) followed and then ACN–MeOH 70 : 30 (v/v) with extracted features of the highest abundance in the Mitra and Capitainer. ACN was the least effective solvent for all the BμS devices. It should be noted that apart from the lowest number of features, Whatman yielded also lower features intensities than both Mitra and Capitainer, regardless of the solvent used which could limit the coverage in metabolite information.

As a means to examine characteristics of precision per extraction condition if any, features intensities RSDs in the triplicate injections were calculated per solvent. The RSD distribution of the different solvents in all the BμS devices were not vastly different. However, there were slight differences. For Whatman, ACN–MeOH 70 : 30 (v/v) had the lowest mean RSD (35.28%), followed by MeOH (49.17%), ACN (45.26%) and MeOH–H_2O 60 : 40 (v/v) (51.89). MeOH–H_2O 60 : 40 (v/v) was the most reproducible solvent for Capitainer (RSD = 34.51%), followed by ACN (40.57%), MeOH (47.08%) and ACN–MeOH 70 : 30 (v/v) (51.71%). Likewise, MeOH–H_2O 60 : 40 (v/v) provided the lowest RSDs for Mitra (RSD = 38.57%), closely followed by ACN (42.65%), MeOH (44.14%) and ACN–MeOH 70 : 30 (v/v) (49.14%). Thus, no specific trend was observed per extraction solvent regarding reproducibility of the acquired metabolic fingerprint. The mean features RSD per solvent and device is represented with a color gradient scale in Fig. 3.

Summarizing, MeOH proved to be the most appropriate extraction solvent for the different BμS devices, as it yields the largest features abundance, high number of features, and comparable RSD distribution with the other solvents. ACN–MeOH 70 : 30 (v/v), which also showed good results, was a close second. Neat ACN and MeOH–H_2O 60 : 40 (v/v) showed the poorest performing results when evaluating all the aforementioned criteria. Therefore, MeOH was selected as the optimum extraction solvent for use in the BμS and plasma comparison study.

3.3 Venous BμS in different devices *versus* plasma

3.3.1 Metabolic coverage. For practical reasons standardized surrogates of BμS were used by applying a defined volume of venous whole blood onto Whatman cards or devices. By this way a higher number of BμS, collected under controlled sampling could be studied, to compare the global metabolic profiles between the three BμS and the most widely used blood type in metabolomics studies, namely plasma. A

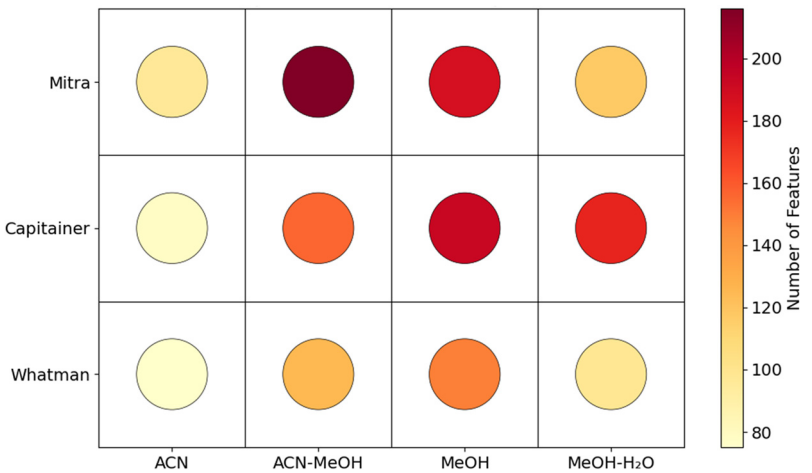

Fig. 2 Number of detected features corresponding to metabolic information obtained from each BμS device using different extraction solvents: ACN, ACN–MeOH 70 : 30 (v/v), MeOH, and MeOH : H_2O 60 : 40 (v/v). Abundance in color (white to red) corresponds to increase in the number of detected features.

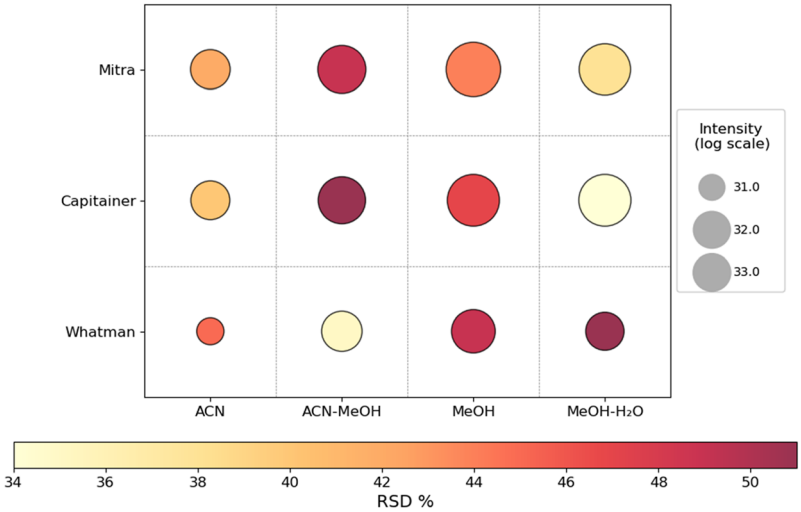

Fig. 3 Summed intensities of the features per extract and microsampling devices and mean RSD in the triplicates. The size of the nodes represents the total abundance of all features in logarithmic scale, whilst the color abundance represents the mean RSD per condition.

set of 10 venipuncture blood samples collected on the three BμS devices and the paired plasma samples were extracted using the defined optimum extraction solvent (MeOH). After the data was normalized using a QC-based linear model in the QC MXP software, they were examined under comparison criteria between the four matrices (three BμS devices and plasma) including total number of features detected, features mean abundance, and number and abundance of annotated metabolites.

After normalization was performed, no significant signal variation was present, as shown by the QC's correlation value (R^2 = 0.994). The variation of IS pentadecane and myristic acid d_{27}, together with other quality assurance analysis can be found in SI Table S4. Regarding the number of features detected per matrix after being processed separately, all four presented a very similar features count: plasma yielded 118, Whatman 119, Mitra 117, and Capitainer 112.

The intensities of the features were also quite similar between the different types of samples. Mitra had the highest mean abundance while plasma had the lowest. Boxplots in Fig. 4 displaying the log2 average peak area of each feature in each matrix show a very similar distribution of features intensities per sample type extracts.

Next, we evaluated the peak area (abundance) of the annotated metabolites per extract. The results of the abundance of the annotated metabolites per condition can be seen in Fig. 5 in the form of a heatmap, where the median of each annotated metabolite across the ten healthy individual samples in each device and plasma is illustrated. Mitra showed to have the highest median abundance in most compound classes (amino acids, fatty acids, organic acids and others), followed closely by Capitainer, which presented higher abundance for the sugars. Overall, Whatman displayed lower abundance for most annotated metabolites compared to the other BμS devices with the

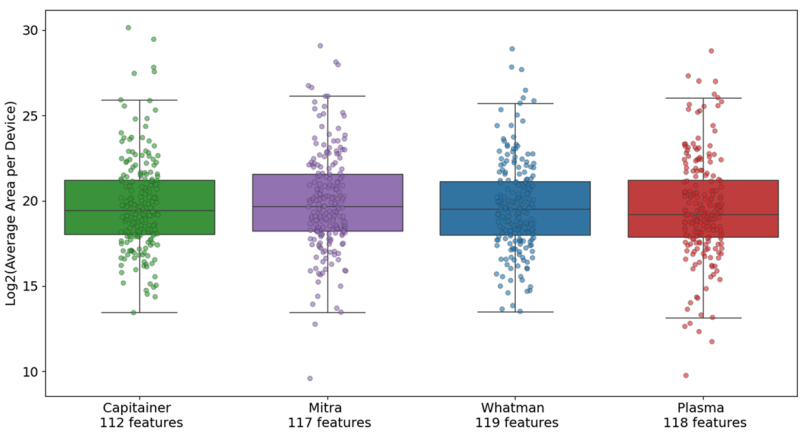

Fig. 4 Boxplots showing the mean log2 peak areas of each feature detected in the four different matrices after extraction with methanol. The lines in each box represent the median peak area, while the dots represent the features.

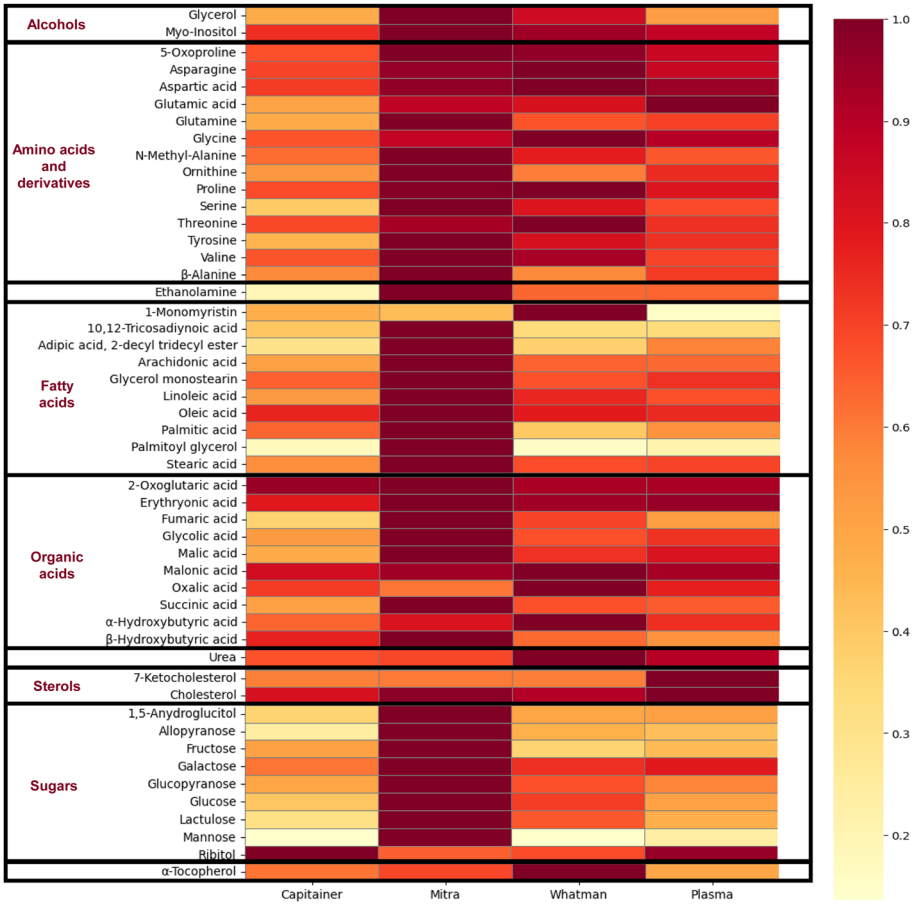

Fig. 5 Median abundance of each metabolite in the extracts from four different types of samples. Color indicates increase in abundance (yellow to red: lowest to highest).

exception of isoleucine, glycerol monostearin, and palmitoyl glycerol.

3.3.2 Metabolic information acquired. The obtained metabolic fingerprints were analyzed by multivariate techniques to explore major trends among the different sampling approaches and understand the potential of the BμS to provide information on a biological question.

After excluding features with >30% CV in the QCs from the normalized data (normalized raw data was log2-transformed and average of the individual triplicates was used) an unsupervised principal component analysis (PCA) of the four matrices was performed with pareto scaling. Missing values were imputed using the k Nearest Neighbors (kNN) method (k = 3). The PCA showed clear discrimination between the four matrices as can be seen in Fig. 6. The R^2 value of the model was 0.702 and the Q^2 value was 0.351. Hoteling's T2 test identified one sample (Capitainer, individual 7), as an outlier. To assess this outlier's influence on the data, the model was repeated excluding this measurement, which rendered no significant alteration on the clustering of the groups, or on the R^2 and Q^2 values. Plasma showed to clearly differ from the BμS matrices as seen on principal component 1 (R^2X[1] 0.293) indicating the different information captured. Mitra device also

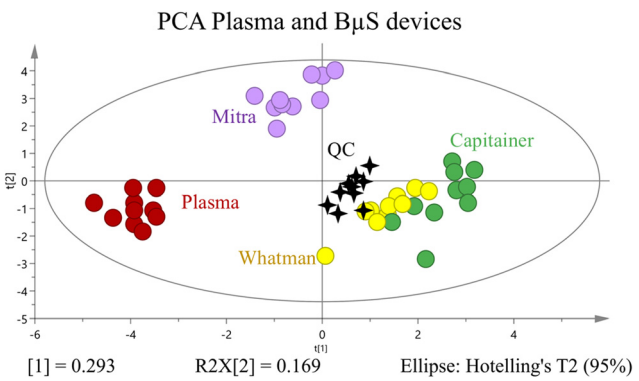

Fig. 6 PCA plot projecting metabolic profiles of plasma and the paired BμS extracts. BμS provide different profiles when compared to plasma. Mitra also exhibits distinct profiles away from Capitainer and Whatman while the latter two had some overlap. R^2 = 0.702 and Q^2 = 0.35.

showed to have a more distinct profile in comparison to the other two BμS matrices as seen on principal component 2 (R^2X[2] 0.169). Capitainer and Whatman clusters had an overlap indicating similarity in their metabolic profiles, something that can be expected due to the same nature of the

material used. Further inspection of m/z over RT features plots (see Fig. S2) of the four matrices confirmed the PCA results shown in Fig. 6.

These findings differ in certain aspects from our previous results.[16] In our earlier similar work where the extracts were analysed using a LC-QTOF platform, plasma was also clustered separately from BμS, illustrating the inherent differences between the matrices. However, Mitra and Whatman had more similar profiles to each other, while Capitainer's Metabolic profiles were clearly different. This evidence shows how GC-MS reveals different facets of metabolic information compared to LC-based approaches.

Another factor that may contribute to the differentiation between the groups is variation in matrix composition. In this study, blank subtraction was performed to remove potential contaminants originating from the BμS devices. Evaluating and accounting for contaminant signals from BμS devices is crucial when applying these technologies in real-world analyses.

To identify the contributing metabolites in the differentiation among plasma and BμS, supervised partial least squares discriminant (PLS-DA) analysis was performed. The PLS-DA models showed clear discrimination between plasma and every BμS device, confirming significant differences in the metabolic profiles. All PLS-DA models were valid with an ANOVA $p < 0.05$, R^2 (model goodness) > 0.5 and Q^2 (model predictability) and $R^2 > Q^2$ (see Fig. S3).

From each of the PLS-DA models (plasma *vs*. Mitra, plasma *vs*. Whatman, and plasma *vs*. Capitainer) features with variable importance projection (VIP) scores > 1, p (correlation) $\geq |0.5|$ and $p[1]$ (covariance) $\leq |0.5|$ were found. Next, T-TEST analysis was performed (2-tailed and assuming unequal variance) and the p values were adjusted for multiple hypothesis testing using the BKY method with a desired FDR rate of 0.5%. Features with q (adjusted p values) < 0.004 were matched with those that passed the first three criteria detailed above and were, therefore, determined to be statistically significant in the discrimination of the matrices.

Based on these models it was found that 22 metabolites differed significantly between plasma and Capitainer. From these, 7 could be annotated. Asparagine, mannose, galactose, glutamine, β-alanine and 7-ketocholesterol had higher abundance in plasma, while 10,12-Tricosadiynoic acid was higher in Capitainer. In the other case between plasma and Mitra, 25 features were significantly different and of these, 10 were annotated. Glutamic acid, cholesterol and 7-ketocholesterol were higher in plasma, while erythronic acid, malic acid, malonic acid, glutamine, aspartic acid, myo-inositol and β-alanine were higher in Mitra. Lastly, between plasma and Whatman, there were 18 discriminant features, from which 6 could be annotated. Cholesterol, malic acid, erythronic acid, β-alanine and 7-ketocholesterol had a higher median in plasma, while 10,12-Tricosadiynoic acid was higher in Whatman. When comparing all these metabolites that differentiate between plasma and the various BμS, six of those metabolites, β-alanine, 7-ketocholesterol, and four unknowns were common in all three pair comparisons. In the upset plot shown in Fig. S4 the number of common annotated metabolites that differed in the three pair comparisons (plasma *vs*. various BμS) are summarized.

These results are not fully aligned with those published in a similar study by Drolet *et al.*,[21] where all annotated metabolites were detected in plasma, but some were missing in venous DBS including adenosine triphosphate (ATP), 5-methyltetrahydrofolic acid, iso-citrate, and other phosphates. In the current study, the reported as missing in DBS extract in comparison to plasma by Drolet *et al.*, were not detected at all, though the extraction solvent was the same. In contrast, the captured information was very similar in all four extracts, all annotated metabolites were identified in all four matrices albeit at different abundance. Most of the unknowns were present in all the matrices, as it can be seen on the similar features number of each BμS device. Given that in the previous study no storage time was defined, this may have had an impact on the results as the samples of the current study had been in storage at −80 °C for more than 6 months.

Lastly, we evaluated the ability of each of the matrices to capture sex-oriented metabolites using PCA. No clear classification based on sex was observed in any of the matrices as seen in Fig. S5, however there is a slight separation in Mitra and plasma in the first two components $R^2[X1] = 0.293$ and $R^2[X2] = 0.169$. In previous works where Volani *et al.*[14] had compared sex metabolic profiles using capillary blood collected on Mitra, venous blood collected on Mitra and plasma, differences were seen. In that study, gluconic acid, an intracellular metabolite[31] showed significantly higher concentrations in males in Mitra compared to plasma. Other metabolites including citrulline, aspartic acid, and *s*-adenosyl-homocysteine, though not at a significant abundance, after multiple hypothesis testing, showed the same trend.

3.4 Capillary BμS device *vs*. whole blood and plasma

The findings presented above are based on the analysis of venous BμS extracts, due to the inherent limitation to acquire multiple samples from fingertips to study experimental parameters. Although this does not fully replicate the clinical conditions of fingerstick sampling, venous BμS serves as a practical and standardized surrogate for early-phase studies. The findings provide information on the effect of the material used and the drying step and knowledge on the differences in abundance seen in plasma *versus* whole blood at given conditions in healthy individuals. Further analysis was therefore conducted to compare the overall untargeted profile obtained by capillary blood sampled with the BμS over liquid whole blood and plasma. Given that Mitra provided satisfactory results in terms of both data richness and its ability to explain biological variation, further study was conducted using Mitra devices in a "real-world application" by collecting blood from fingertips.

Unlike the previous analyses, this dataset was processed using XCMS due to data format incompatibilities. It is important to note that, as this was an independent analysis, the use

of a different software platform does not affect the interpretation of the results. A PCA model that was constructed and is provided in Fig. S6 showed that the three matrices differ to a considerable extent across t1 with an explained variation of 57% ($R^2X[1] = 0.57$).

As it was expected, greater difference was observed between BμS and plasma, whereas whole blood is in between. The metabolic profiles of the Mitra for all three individuals is however still distinct from their paired venous liquid blood. Differences due to variation of some metabolites abundance in capillary blood when compared to venous blood but also due to instability or stability of metabolites after the drying step should be considered. The effect of EDTA anticoagulants used in whole blood and plasma should also not be disregarded as it may alter the acquired metabolic profiles.[32]

Univariate analysis was performed in pairs for all three individuals to compare the signals in the three different matrices. Features were considered when the ratio to blank was higher than 20 and statistically significant metabolites were considered when the p value was below 0.05 and if they passed the Benjamini, Krieger and Yekutieli False Discovery Rate test. Based on these criteria, 23 metabolites were found statistically relevant for the separation between whole blood and Mitra in two out of the three tested individuals.

Out of these, 14 metabolites were found at higher abundance in Mitra in all 3 individuals compared to blood or plasma (see Fig. 7). These include seven aminoacids and derivatives such as serine, valine, asparagine, aspartic acid, glutamic acid, ornithine and threonine, fatty acids such as palmitic, oleic and stearic acids as well as cholesterol and gly-

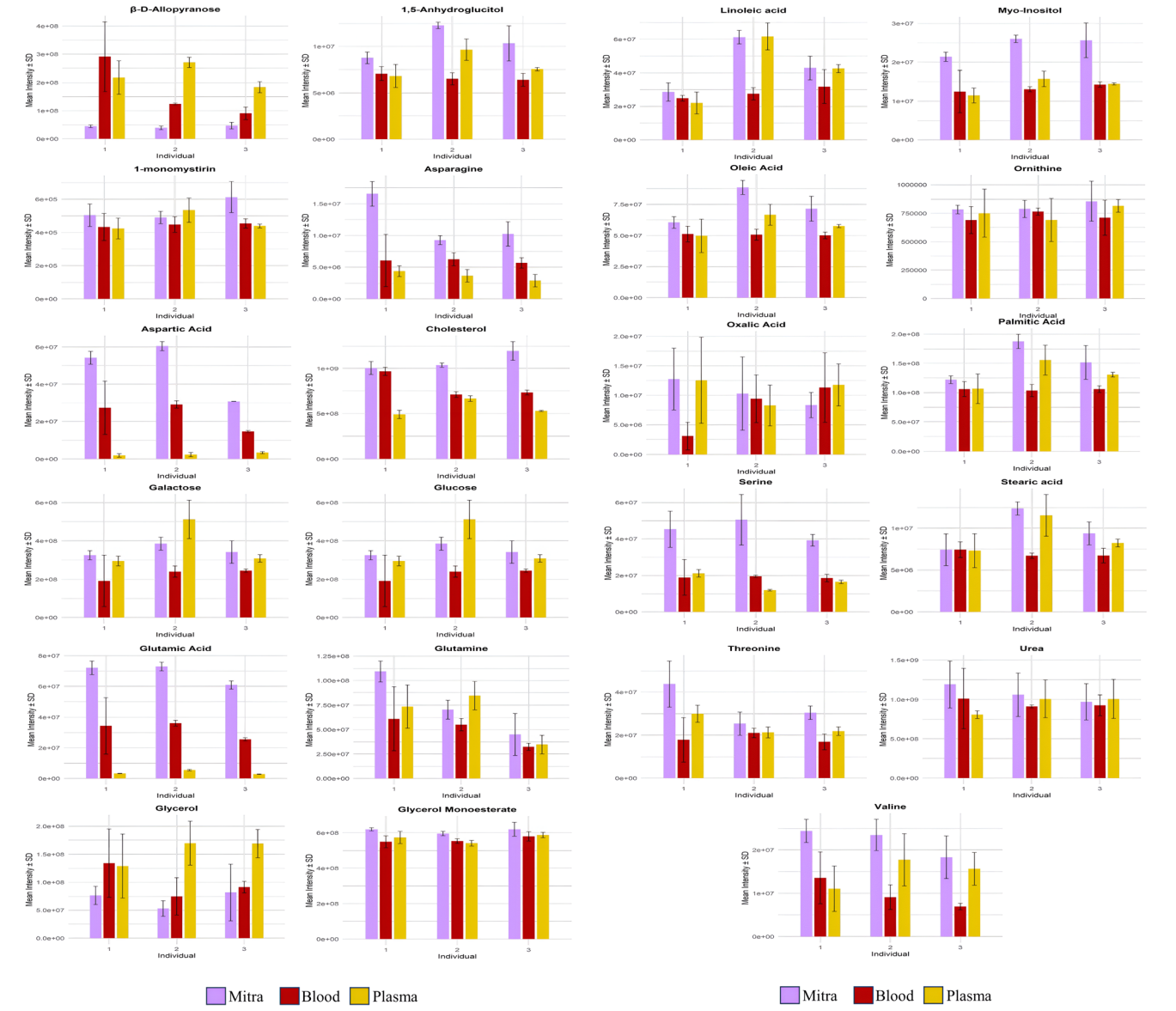

Fig. 7 Abundance of metabolites found to differ between Mitra capillary blood collected from the finger tip of three healthy individuals and their paired blood and plasma samples.

cerol. 1,5-Anhydroglucitol and myo-inositol were also found at higher abundance in the Mitra extracts compared to the other blood samples.

In some other cases such as the β-allopyranose and glycerol, the abundance was found lower in Mitra extracts.

Among the significantly different signals revealed by the statistical analysis was also EDTA which was absent in Mitra and present in both blood and plasma (much lower in whole blood).

There were also metabolites that did not show a constant trend in all three individuals, such as glucose, urea, oxalate and monomystirin.

The observed differences between venous blood and BμS profiles apart from artifacts induced by the BμS device itself, may also arise from inherent biological differences between venous and capillary blood. Indeed, capillary blood, which bridges arterial and venous circulation, has a composition distinct from both—though more similar to arterial blood. As well as that, interstitial and intracellular components are also inevitably acquired when collecting capillary blood, and might also interfere with the overall metabolic profiles.[33]

Overall, capillary blood remains a relatively underexplored matrix compared to conventional specimens such as plasma and venous blood, particularly with respect to global metabolite profiling. Reference concentration ranges of metabolites in capillary blood are less well established. There are reports of specific cases of metabolites such as glucose which is found in higher concentrations in capillary blood compared to liquid venous blood;[34] urea was reported to have similar concentration levels in capillary and venous serum.[35] However no bridging data in large cohorts for various metabolites exist.

The glucose trend found in our study agrees with the previous report, while urea did not show a constant trend among the three individuals as can be seen in Fig. 7.

A notable difference was observed for a few metabolites *e.g.* glutamate, aspartate, valine, serine and myoinositol whose abundance was double or even more in Mitra (in all three individuals) compared to blood. This could be explained by the similarity of capillary to arterial blood which often contains higher concentrations of certain metabolites, such as amino acids. In a paired arterial and venous plasma study from 20 healthy individuals, arterio–venous differences from fold change 1 (valine, serine) to up to 3 (glutamate) have been shown for amino acids.[36] In addition, as myo-inositol is also taken up by peripheral tissues such as muscle and skin, it is expected to be lower in venous blood—collected downstream of these tissues. It should be noted that when venous Mitra was compared with plasma above (paragraph 3.3), some of these metabolites were not found to differ, while *e.g.* for glutamate the opposite trend was observed (lower in venous Mitra than in plasma).

In general, differences were also observed between blood and plasma for the aforementioned metabolites, varying by individual. This indicates that metabolite abundance is influenced by both individual metabolite state and metabolite function. Studies with larger cohorts of healthy individuals are therefore essential to draw robust conclusions.

When comparing plasma and Mitra, 67 compounds were found to be statistically different in the three pair comparisons of the individuals. As expected, the number of differentiating metabolites for these two matrices was greater in comparison to whole blood comparison which was besides shown by PCA (Fig. S5).

In an upcoming study involving more than 20 healthy individuals, where paired plasma and fingertip Mitra samples are being collected, we plan to further evaluate and validate the findings reported here.

4 Conclusions

Our study demonstrates that BμS represents a robust and practical surrogate for blood and plasma in GC-MS metabolomic profiling, achieving a remarkably comparable metabolite coverage with only minimal losses. This establishes BμS as a viable and powerful alternative, particularly given its substantial advantages in ease of collection, reduced invasiveness and simplified logistics. Yet, it should be noted that certain metabolites may be underrepresented in dried matrices, highlighting the importance of careful validation when specific compounds are critical to a study.

Importantly, next-generation microsampling devices such as Mitra and Capitainer have proven capable of delivering information equal to, or in some cases surpassing, that obtained from conventional plasma samples. While these devices inevitably generate data that differ from plasma and whole blood profiles, owing both to the dried *versus* liquid matrix and the inclusion of cellular metabolites, they open new analytics windows that extend beyond the scope of traditional sampling.

These findings underline a key message: BμS is not merely a substitute for plasma but a distinct and highly valuable matrix that can transform metabolomics workflows. With careful, application-specific validation, BμS could reshape clinical and translational research, expanding metabolomics into settings where traditional sampling is impractical or impossible.

Author contributions

Conceptualization: Helen Gika; resources: Daniel Marques de Sá e Silva, Marlene Thaitumu, Helen Gika, Georgios Theodoridis; methodology: Helen Gika, Daniel Marques de Sá e Silva, Marlene Thaitumu, Christina Virgiliou; investigation: Daniel Marques de Sá e Silva, Marlene Thaitumu; data curation: Daniel Marques de Sá e Silva, Marlene Thaitumu; formal analysis: Daniel Marques de Sá e Silva, Marlene Thaitumu, Alexandra Tiganouria; writing – original draft preparation: Daniel Marques de Sá e Silva, Marlene Thaitumu, Helen Gika; writing – review, and editing: Daniel Marques de Sá e Silva, Marlene Thaitumu, Helen Gika, Christina Virgiliou, Georgios Theodoridis, and Fernanda Rey-Stolle; supervision by Helen

Gika and Georgios Theodoridis. All authors have read and agreed to the published version of the manuscript.

Conflicts of interest

The authors have no competing interests to declare that are relevant to the content of this article.

Institutional review board statement

All experiments were performed in accordance with the guidelines of the Declaration of Helsinki. The study was approved by the Research Ethics Committee of the Aristotle University of Thessaloniki (#306272/2022).

Informed consent statement

Informed consent was obtained from all subjects involved in the study.

Data availability

Data for this article, including raw and processed spectral data, are available at MassIVE repository, under the ID **MassIVE MSV000099001** and is available at https://doi.org/doi:10.25345/C5DR2PN68.

Supplementary information (SI) is available. Fig. S1 Common and unique features from each BμS device using different extraction solvents. Fig. S2 Plot of retention time vs m/z from the GC-MS analysis of the four different extracts from 10 individuals. Fig. S3 PLS-DA models showed clear discrimination between plasma and every BμS device. Fig S4 Upset plot showing common annotated metabolites that differentiate plasma from various BμS. Fig. S5 PCA models of metabolome classification based on sex in the four extracts. Fig. S56 PCA plot analyzing metabolic profiles of plasma, whole blood and Mitra BμS devices. Supplementary Table S1 – FAMES RI. Supplementary Table S2 – Liquid blood annotations. Supplementary Table S3 – QA Solvent Optimization. Supplementary Table S4 – QA Device Comparison. See DOI: https://doi.org/10.1039/d5an00937e.

Acknowledgements

This work was supported by the HUMAN HORIZON-MSCA-2021-DN. The project was funded by The European Union Horizon 2020, Marie Curie Actions, grant number 101073062.

References

1 I. Gertsman and B. A. Barshop, *J. Inherited Metab. Dis.*, 2018, **41**, 355–366.
2 H. Gika, G. Theodoridis, R. S. Plumb and I. D. Wilson, in *Liquid Chromatography (Third Edition)*, ed. S. Fanali, B. Chankvetadze, P. R. Haddad, C. F. Poole and M.-L. Riekkola, Elsevier, 3rd edn, 2023, vol. 2, pp. 403–429.
3 E. Bossi, E. Limo, L. Pagani, N. Monza, S. Serrao, V. Denti, G. Astarita and G. Paglia, *Metabolites*, 2024, **14**(1), 46.
4 G. Nys, M. G. M. Kok, A. C. Servais and M. Fillet, *TrAC, Trends Anal. Chem.*, 2017, **97**, 326–332.
5 V. Londhe and M. Rajadhyaksha, *J. Pharm. Biomed. Anal.*, 2020, **182**, DOI: 10.1016/j.jpba.2020.113102.
6 M. T. Ackermans, V. de Kleijne, F. Martens and A. C. Heijboer, *Clin. Chim. Acta*, 2021, **520**, 179–185.
7 H. B. Wang, X. Xiao, X. Y. He and S. T. Wang, *Talanta*, 2024, **278**, DOI: 10.1016/j.talanta.2024.126491.
8 N. Spooner, *Bioanalysis*, 2015, **7**, 1971–1976.
9 E. E. Balashova, O. P. Trifonova, D. L. Maslov and P. G. Lokhov, *Health Prim. Care*, 2018, **2**(5), 1–11.
10 D. M. S. Silva, M. Thaitumu, G. Theodoridis, M. Witting and H. Gika, *Metabolites*, 2023, **13**(10), 1038.
11 H. Nishio, S. Kodama, S. Yokoyama, T. Matsuo, T. Mio and K. Sumino, *Clin. Chim. Acta*, 1986, **159**, 77–82.
12 R. Zakaria, K. J. Allen, J. J. Koplin, P. Roche and R. F. Greaves, *eJIFCC*, 2016, **27**(4), 288–317.
13 N. H. Tobin, A. Murphy, F. Li, S. S. Brummel, T. E. Taha, F. Saidi, M. Owor, A. Violari, D. Moodley, B. Chi, K. D. Goodman, B. Koos and G. M. Aldrovandi, *Metabolomics*, 2021, **17**(62), DOI: 10.1007/s11306-021-01813-3.
14 C. Volani, C. Malfertheiner, G. Caprioli, S. Fjelstrup, P. P. Pramstaller, J. Rainer and G. Paglia, *Metabolites*, 2023, **13**(2), 146.
15 X. Shen, R. Kellogg, D. J. Panyard, N. Bararpour, K. E. Castillo, B. Lee-McMullen, A. Delfarah, J. Ubellacker, S. Ahadi, Y. Rosenberg-Hasson, A. Ganz, K. Contrepois, B. Michael, I. Simms, C. Wang, D. Hornburg and M. P. Snyder, *Nat. Biomed. Eng.*, 2024, **8**, 11–29.
16 M. N. Thaitumu, D. M. S. Silva, P. Louail, J. Rainer, G. Avgerinou, A. Petridou, V. Mougios, G. Theodoridis and H. Gika, *Metabolites*, 2025, **15**(1), 62.
17 E. Bossi, S. Serrao, P. Reveglia, A. Ferrara, M. Nobile, E. Limo, G. Corso and G. Paglia, *Anal. Bioanal. Chem.*, 2025, **417**, 1791–1805.
18 S. T. Kong, S. H. Lim, J. Ching and P. C. L. Ho, *J. Pharm. Biomed. Anal.*, 2025, **253**, DOI: 10.1016/j.jpba.2024.116561.
19 H. N. Cui, F. Shi, G. Huang, Y. He, S. Yu, L. Liu, Y. Li and H. Wen, *Sci. Rep.*, 2024, **14**, 30964.
20 M. P. Cala and R. J. W. Meesters, *Bioanalysis*, 2017, **9**, 1329–1340.
21 J. Drolet, V. Tolstikov, B. A. Williams, B. P. Greenwood, C. Hill, V. K. Vishnudas, R. Sarangarajan, N. R. Narain and M. A. Kiebish, *Metabolites*, 2017, **7**, 35.
22 S. T. Kong, H. S. Lin, J. Ching and P. C. Ho, *Anal. Chem.*, 2011, **83**, 4314–4318.
23 S. Kumari, D. Stevens, T. Kind, C. Denkert and O. Fiehn, *Anal. Chem.*, 2011, **83**, 5895–5902.

24 O. Fiehn, *Curr. Protoc. Mol. Biol.*, 2016, **114**, 30.4.1–30.4.32.
25 M. Ioannidis, T. Mouskeftara, E. Iosifidis, M. Simitsopoulou, E. Roilides, H. Gika, M. F. Rey-Stolle and C. Virgiliou, *J. Chromatogr. A*, 2025, **1753**, DOI: 10.1016/j.chroma.2025.465924.
26 P. Louail, A. Tagliaferri, V. Verri Hernandes, D. M. S. Silva, M. De Graeve and J. Rainer, rformassspectrometry/Metabonaut: v1.2.0, *Zenodo*, 2025, DOI: 10.5281/zenodo.15190305.
27 D. Broadhurst, *broadhurstdavid/QC-MXP: QC:MXP version 2.0*, 2025, DOI: 10.5281/zenodo.15233092.
28 Y. Benjamini and Y. Hochberg, *J. R. Stat. Soc. Ser. B Methodol.*, 1995, **57**, 289–300.
29 L. W. Sumner, A. Amberg, D. Barrett, M. H. Beale, R. Beger, C. A. Daykin, T. W. M. Fan, O. Fiehn, R. Goodacre, J. L. Griffin, T. Hankemeier, N. Hardy, J. Harnly, R. Higashi, J. Kopka, A. N. Lane, J. C. Lindon, P. Marriott, A. W. Nicholls, M. D. Reily, J. J. Thaden and M. R. Viant, *Metabolomics*, 2007, **3**, 211–221.
30 A. I. Ruiz-Matute, O. Hernández-Hernández, S. Rodríguez-Sánchez, M. L. Sanz and I. Martínez-Castro, *J. Chromatogr. B*, 2011, **879**(17–18), 1226–1240.
31 Ó. Rolfsson, G. Paglia, M. Magnusdóttir, B. Palsson and I. Thiele, *Biochem. J.*, 2013, **449**, 427–435.
32 J. W. Lee, *Bioanalysis*, 2014, **6**(8), 1037–1040.
33 C. McNamara, *Dacie and Lewis Practical Haematology*, Elsevier Inc., 12th edn, 2017, pp. 1–7.
34 K. Kuwa, T. Nakayama, T. Hoshino and M. Tominaga, *Clin. Chim. Acta*, 2001, **307**, 187–192.
35 I. R. Kupke and S. Zeugner, *Clin. Chim. Acta.*, 1981, **112**, 177–185.
36 J. Ivanisevic, D. Elias, H. Deguchi, P. M. Averell, M. Kurczy, C. H. Johnson, R. Tautenhahn, Z. Zhu, J. Watrous, M. Jain, J. Griffin, G. J. Patti and G. Siuzdak, *Sci. Rep.*, 2015, **5**, DOI: 10.1038/srep12757.